

---

# Two is better than one: A Collapse-free Multi-Reward RLIF Training Framework

---

Shourov Joarder<sup>1</sup> Diganta Sikdar<sup>1</sup> Ahsan Habib Akash<sup>2</sup>  
 Binod Bhattarai<sup>3,4,5</sup> Prashna Gyawali<sup>2\*</sup>

<sup>1</sup>Bangladesh University of Engineering and Technology, Bangladesh

<sup>2</sup>West Virginia University, USA <sup>3</sup>University of Aberdeen, UK <sup>4</sup>Fogsphere (Redev.AI Ltd, UK)

<sup>5</sup> University College London, UK

## Abstract

Reinforcement learning with verifiable rewards (RLVR) has substantially improved the reasoning ability of LLMs, but often depends on external supervision from human annotations or gold-standard solutions. Reinforcement learning from internal feedback (RLIF) has recently emerged as a scalable unsupervised alternative, using signals extracted from the model itself. However, existing RLIF methods typically rely on a single internal reward, which can lead to reward hacking, entropy collapse, and degraded reasoning structure. We propose a multi-reward RLIF framework that decomposes the training signal into two complementary components: an answer-level reward based on cluster voting and a completion-level reward based on token-wise self-certainty. To combine these signals robustly, we apply GDPO-based normalization to reduce reward-scale imbalance. We further introduce KL-Cov regularization, which targets low-entropy token distributions responsible for disproportionate entropy reduction, preserving exploration and preventing late-stage collapse. Across mathematical reasoning and code-generation benchmarks, our method improves stability and robustness over prior unsupervised RL approaches, while achieving performance close to supervised RLVR methods. These results show that complementary internal rewards, combined with targeted regularization, can support stable long-horizon reasoning without relying on external ground-truth supervision. Code will be released soon.

## 1 Introduction

Large language models (LLMs) have achieved striking success across domains, yet training them to reason through complex problems remains an open and central challenge in modern AI. Reinforcement learning with verifiable rewards (RLVR) has emerged as a powerful paradigm, enabling models such as DeepSeek-R1 [DeepSeek-AI, 2025] and MiMo [Xiaomi LLM-Core Team, 2025] to attain strong mathematical reasoning through reward signals derived from ground-truth answer verification. However, RLVR critically depends on external supervision such as human-labeled reasoning traces, verified reference answers, or pre-trained reward models which limits scalability and practical applicability across domains where such supervision is unavailable, costly, or difficult to obtain.

Reinforcement Learning with Internal Feedback (RLIF) offers an unsupervised alternative that eliminates the need for external supervision entirely. Instead of relying on ground-truth labels, RLIF methods derive reward signals solely from intrinsic model signals: either through consensus-based measures such as majority voting and semantic clustering [Zhang et al., 2025a], or through entropy minimization measures such as the self-certainty score [Zhao et al., 2025b]. These approaches have

---

\*Correspondence to prashna.gyawali@mail.wvu.edu.

demonstrated that meaningful reasoning improvements are achievable without labeled data, making them a promising path toward scaling LLM reasoning to arbitrary domains [Zuo et al., 2025, Zhao et al., 2025a, Prabhudesai et al., 2025].

Despite these promising results, existing RLIF methods exhibit recurring failure patterns, including reward hacking and model collapse [Agarwal et al., 2025, Prabhudesai et al., 2025]. Prior work has observed that models often achieve strong initial gains but gradually degrade after extended training. We argue that this decline stems from the structure of the reward signals themselves. For example, self-certainty rewards high-confidence token distributions, effectively using entropy minimization as a proxy for output quality. Majority voting, though consensus-based rather than explicitly entropy-driven, similarly favors outputs that the model already assigns high probability to, thereby indirectly reinforcing low-entropy behavior. Under both signals, the policy is incentivized to reduce token-level uncertainty, whether or not this reduction improves reasoning quality.

This incentive creates two compounding failure modes. First, high-entropy transitional tokens, such as *however*, *thus*, *because*, and *suppose*, which often serve as structural anchors in chain-of-thought reasoning, are disproportionately penalized [Zhang et al., 2025b]. This can weaken logical coherence even when final-answer accuracy temporarily improves. Second, because shorter responses contain fewer uncertain tokens, the reward implicitly favors brevity over depth [He et al., 2026], encouraging terse, high-probability outputs rather than genuine improvements in reasoning quality. This pattern of early improvement followed by degradation is an empirical instance of Goodhart’s Law [Gao et al., 2022]: when a single proxy becomes the sole optimization target, the policy learns to exploit the proxy rather than improve the underlying capability. As optimization proceeds, the reward signal and true task performance can decouple, leading to overoptimization.

This motivates a multi-reward RLIF objective that jointly optimizes structurally complementary signals rather than relying on a single proxy. Specifically, we propose a multi-reward RLIF framework that combines answer agreement and model confidence as intrinsic rewards. We then introduce a targeted regularization strategy to reduce collapse during optimization. To prevent either reward from dominating optimization, we normalize the advantages induced by each reward independently. We further introduce a targeted regularization strategy to reduce collapse during optimization. In particular, to mitigate entropy collapse while preserving exploration, we use KL-Cov regularization, inspired by Cui et al. [2025], which targets the small subset of tokens responsible for disproportionate entropy reduction while maintaining diversity in the remaining token distribution. Across five diverse mathematical reasoning benchmarks and two coding benchmarks, we show that our method outperforms several baselines, including single-reward RLIF frameworks such as self-certainty and majority voting Zhao et al. [2025b], Zuo et al. [2025] while maintaining stable gains under continued training. This stability is crucial for RLIF: as models scale and reasoning trajectories grow more complex, training must preserve exploration beyond early high-confidence behaviors rather than collapse into narrow reward-seeking patterns.

Our contributions can be summarized as follows:

- We propose a multi-reward RLIF framework with GDPO normalization that jointly optimizes answer-level consensus and completion-level self-certainty, mitigating the failure modes of single-proxy optimization.
- We utilized KL-Cov regularization to the unsupervised multi-reward setting as a targeted policy constraint to high-covariance entropy-collapsing tokens while preserving exploration over the remaining token distribution.
- Across five mathematical reasoning benchmarks and two coding benchmarks, we show that our method improves performance over single-reward RLIF baselines and remains stable under continued training.

## 2 Related Work

**Reinforcement learning with internal feedback (RLIF).** To eliminate external supervision, recent work has explored RLIF, where the model’s own predictions serve as the reward signal. INTU-ITOR [Zhao et al., 2025b] uses the average KL divergence between a uniform distribution and the model’s next-token distribution as a self-certainty score, rewarding more confident reasoning traces. EMPO [Zhang et al., 2025a] takes a complementary approach, employing entropy minimization by

semantically clustering rollout answers and rewarding rollouts proportionally to their cluster size. TTRL [Zuo et al., 2025] shows that majority voting yields surprisingly effective rewards for test-time RL without ground-truth labels. Absolute Zero [Zhao et al., 2025a] and R-Zero [Huang et al., 2025] propose self-play frameworks where models generate their own training tasks, removing the need for curated datasets entirely. Zhou et al. [2025] extend RL-based reasoning to general domains without verifiers by maximizing the probability of generating reference answers. Co-rewarding [Zhang et al., 2025c] seeks complementary supervision from multiple views to stabilize self-supervised RL, addressing the training collapse that single-view signals cause. SSR-Zero [Yang et al., 2025] extends self-rewarding RL to machine translation, demonstrating that the paradigm generalizes beyond mathematical reasoning. While these methods advance unsupervised RL in various directions, they each rely on a single reward signal or a single feedback mechanism, making them susceptible to the failure modes described in Section 1.

**Entropy minimization, entropy collapse, and model collapse.** Uncontrolled entropy minimization, rewarding more confident outputs to improve reasoning without any labels [Agarwal et al., 2025, Prabhudesai et al., 2025], is also the primary driver of collapse. Chen et al. [2026] formalize how clipping bias under spurious rewards reduces policy entropy, and Cui et al. [2025] show that  $\sim 95\%$  of entropy reduction happens in the earliest training steps, with a tiny  $\sim 0.02\%$  fraction of high-covariance tokens with anomalously large centered cross-products between log-probability and advantage dominating the policy gradient and driving entropy to zero. The downstream pathology is well-documented: Shafayat et al. [2025] report complete model collapse in self-training (identical outputs regardless of input), Zhang et al. [2025b] show that all RLIF approaches exhibit a rise-then-fall trajectory attributable to over-optimization of a single internal signal, and He et al. [2026] confirm this pattern across intrinsic-reward methods at scale, with collapse timing set by model priors.

**Multi-objective RL and reward combination.** Combining multiple reward signals in RL is challenging because naive summation leads to scale dominance, where the reward with larger variance overwhelms the gradient signal. GDPO [Liu et al., 2026] addresses this by normalizing each reward channel independently within groups before combination, ensuring that no single reward dominates purely due to scale differences. Our work builds on the GDPO normalization principle by applying it in the context: combining answer-level and completion-level rewards for unsupervised LLM training, paired with covariance-aware regularization to prevent entropy collapse.

### 3 Method

We present a multi-reward RLIF framework. The framework combines answer-level agreement, completion-level self-certainty, group-wise reward normalization, and covariance-aware regularization within a GRPO-style policy optimization objective.

At a high level, for each prompt  $q$ , our method samples  $G$  completions from the rollout policy  $\pi_{\theta_{\text{old}}}$ . From each completion, we extract the final answer and cluster the resulting answers by equivalence. Each completion is assigned two rewards: an answer-agreement reward determined by the size of its answer cluster, and a completion-level confidence reward computed using self-certainty. We normalize each reward channel within the  $G$ -sample group and form a rollout-level advantage from their weighted sum. The policy is then optimized with a GRPO-style objective, with additional log-ratio regularization applied to high-covariance tokens. Figure 1 illustrates the overall training pipeline.

#### 3.1 Preliminaries

Let  $\pi_{\theta}$  denote the current policy,  $\pi_{\theta_{\text{old}}}$  denote the rollout policy used to generate the current training batch, and  $\pi_{\text{ref}}$  denote a frozen reference policy. Given a prompt  $q$ , we sample  $G$  completions from  $\pi_{\theta_{\text{old}}}$ . The  $g$ -th completion is denoted by  $c_g = (c_{g,1}, \dots, c_{g,T_g})$ , where  $T_g$  is its length, and its extracted final answer is denoted by  $a_g$ . During optimization, each token in completion  $c_g$  inherits the rollout-level advantage  $A_g$  computed from the reward signals.

We optimize the policy using a GRPO-style clipped surrogate objective [Shao et al., 2024]. For a generated token  $y_i$  with inherited advantage  $A_i$ , let  $\rho_i = \pi_{\theta}(y_i | q, y_{<i}) / \pi_{\theta_{\text{old}}}(y_i | q, y_{<i})$  be the

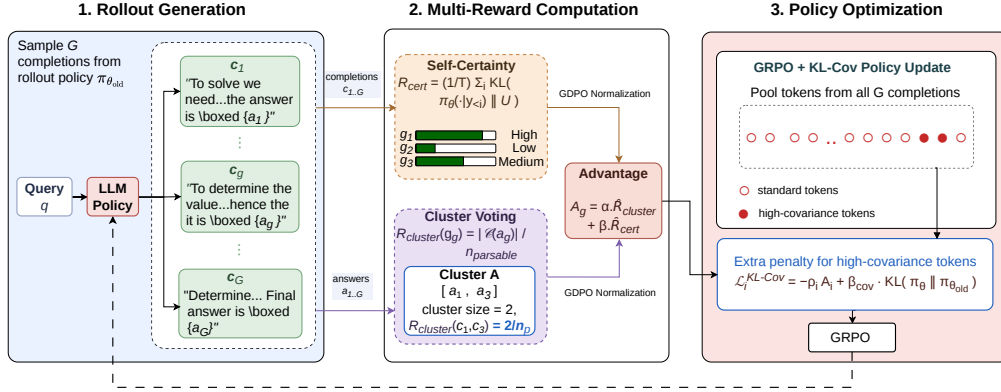


Figure 1: Given a prompt, we sample  $G$  completions from the rollout policy and compute two intrinsic rewards: an answer-level cluster-voting reward over final-answer agreement, and a completion-level self-certainty reward over token-level predictive distributions. Each reward is normalized within the prompt group before being combined into rollout-level advantages. Optimization uses a GRPO-style objective, while KL-Cov penalizes only high-covariance tokens to regularize concentrated updates.

importance sampling ratio between the current and rollout policies. The per-token GRPO loss is

$$\mathcal{L}_i^{\text{GRPO}}(\theta) = -\min\left[\rho_i A_i, \text{clip}(\rho_i, 1-\epsilon, 1+\epsilon) A_i\right] \quad (1)$$

where  $\epsilon > 0$  is the clipping parameter. The following sections describe how we combine multiple unsupervised reward signals and add targeted regularization for high-covariance tokens.

### 3.2 Answer-Level Reward via Cluster Voting

The first reward channel assigns higher reward to completions whose final answers agree with many other sampled completions for the prompt. Given  $G$  rollouts for a prompt  $q$ , we extract the final answers  $a_1, \dots, a_G$  and group them into  $C$  clusters by exact equivalence on the normalized answer string. Rather than binary majority voting, which assigns reward only to the most popular answer, we assign each rollout  $g$  a reward proportional to the fraction with equivalent answers:

$$R_{\text{cluster}}(a_g) = \begin{cases} |\{g' \in \{1, \dots, G\} : a_{g'} \equiv a_g\}| / n_{\text{parseable}} & \text{if } a_g \text{ is parseable,} \\ 0 & \text{otherwise,} \end{cases} \quad (2)$$

where  $n_{\text{parseable}}$  is the number of rollouts (out of  $G$ ) whose answer string parses successfully. For mathematical problems, the equivalence is measured with numerical consistency. This provides a denser signal than binary majority voting: minority clusters receive small but nonzero rewards rather than zero, and this type of clustering is shown to be robust to surface-level variation in equivalent answers [Zhang et al., 2025a, Kuhn et al., 2023]. In implementation, we additionally include a small auxiliary boxed-format reward (weight 0.1) alongside the cluster reward to gate non-parseable completions (reported in Appendix F).

### 3.3 Completion-Level Reward via Self-Certainty

Following Zhao et al. [2025b], we use self-certainty as a completion-level reward. Let  $\mathcal{V}$  denote the vocabulary and let  $\mathcal{U}$  denote the uniform distribution over  $\mathcal{V}$ . For a completion  $c_g = (c_{g,1}, \dots, c_{g,T_g})$ , we compute the self-certainty reward online from the current policy as

$$R_{\text{cert}}(c_g) = \frac{1}{T_g} \sum_{t=1}^{T_g} D_{\text{KL}}(\mathcal{U} \parallel \pi_{\theta}(\cdot \mid q, c_{g,<t})) \quad (3)$$

where  $c_{g,<t} = (c_{g,1}, \dots, c_{g,t-1})$  is the prefix before token  $t$  of generation  $g$ . Used in isolation, self-certainty has been shown to favor degenerate policies that produce overly deterministic or

short templated completions regardless of the input [Shafayat et al., 2025, Zhang et al., 2025b, He et al., 2026]. Our qualitative examples (in Appendix G) shows similar reward-hacking, with self-certainty completions reusing similar tokens across questions. Consistently, our own single-reward decomposition (Figure 3) demonstrate that self-certainty reward alone collapses to  $\sim 100$ -token templates with token-distribution entropy in  $[0.03, 0.17]$ .

This motivates our multi-reward design, which combines self-certainty with cluster voting instead of optimizing either signal alone. These rewards provide complementary signals: self-certainty scores the policy’s confidence during completion generation, whereas cluster voting scores agreement among sampled final answers.

### 3.4 Group-Wise Multi-Reward Normalization

Since the cluster and self-certainty rewards have different numerical scales, cluster voting produces values in  $[0, 1]$  while self-certainty values depend on vocabulary size, naive combination can cause one signal to dominate the advantage purely because of scale and the performance degrades. We confirm this empirically in Appendix E: replacing per-channel  $z$ -scoring with a single combine-then-normalize step degrades downstream accuracy across different datasets (Figure 6), and a logprob-space gradient diagnostic (Figure 7) shows that the higher-variance self-certainty channel dominates the per-token gradient by roughly an order of magnitude whereas the cluster channel is effectively silenced. To avoid this, we normalize each reward channel independently within the group of  $G$  completions for the same prompt, following the GDPO principle [Liu et al., 2026]. For each reward channel  $k \in \{\text{cluster, cert}\}$ , we compute the group mean and standard deviation as  $\mu_k = \frac{1}{G} \sum_{g=1}^G R_k(g)$  and  $\sigma_k = \text{std}(\{R_k(g)\}_{g=1}^G)$ . The normalized reward for rollout  $g$  under channel  $k$  is:

$$\hat{R}_k(g) = \frac{R_k(g) - \mu_k}{\sigma_k + \epsilon} \quad (4)$$

where  $\epsilon > 0$  is a small constant for numerical stability.

We then combine the normalized rewards into a single rollout-level advantage:

$$A_g = \alpha \cdot \hat{R}_{\text{cluster}}(a_g) + \beta \cdot \hat{R}_{\text{cert}}(c_g) \quad (5)$$

where  $\alpha, \beta \geq 0$  are reward weights. The weights  $\alpha$  and  $\beta$  then control the relative importance of answer quality versus reasoning quality. For this study, we empirically set them as  $\alpha = \beta = 0.5$ .

### 3.5 KL-Cov: Covariance-Aware Policy Optimization

We observe that two rewards provide complementary supervision, but each also induces a different degeneration mode when optimized alone. Cluster-only training drifts in answer space, with rising entropy and lengthening completions, while self-certainty collapses token-space entropy, producing peaked distributions and short  $\sim 100$ -token templates (Figure 3). Although GDPO normalization mitigates these instabilities by balancing the two reward channels, the resulting policy remains vulnerable to collapse. In our ablation, the GDPO-normalized combination still degenerates around step 240 when trained without additional exploration regularization (Figure 4).

We therefore require a regularizer that targets the tokens responsible for collapse without unnecessarily constraining the rest of the policy. We therefore adopt KL-Cov: each batch we identify the top- $k$  ( $k=0.02$ ) tokens by covariance and apply a targeted KL penalty only to them, leaving the remaining  $\sim 98\%$  under the standard clipped GRPO surrogate. Using the set of  $N$  batch tokens  $\{y_1, \dots, y_N\}$  defined in Section 3.1, we compute a covariance estimate between token log-probabilities and rollout advantages as the average centered cross-product across tokens:

$$\text{Cov}(y_i) = \left( \log \pi_\theta(y_i | y_{<i}) - \frac{1}{N} \sum_{j=1}^N \log \pi_\theta(y_j | y_{<j}) \right) \cdot \left( A_i - \frac{1}{N} \sum_{j=1}^N A_j \right) \quad (6)$$

A large positive  $\text{Cov}(y_i)$  means that the token is more probable than average and has a higher than average advantage, or that the token is less probable than average and has a lower average advantage. The first scenario encourages entropy collapse and the second scenario basically has no

effective gradient learning. We rank all  $N$  tokens by covariance and select the top- $k$  fraction as the high-covariance set:

$$\mathcal{I}_{\text{KL}} = \{i \in \{1, \dots, N\} \mid \text{Rank}(\text{Cov}(y_i)) \leq k \cdot N\}, \quad k \ll 1 \quad (7)$$

where  $\text{Rank}(\cdot)$  orders tokens from highest to lowest covariance, so rank 1 is the most problematic token. The per-token loss depends on whether the token belongs to  $\mathcal{I}_{\text{KL}}$ :

$$\mathcal{L}(y_i; \theta) = \begin{cases} -\min[\rho_i A_i, \text{clip}(\rho_i, 1-\epsilon, 1+\epsilon) A_i] & \text{if } i \notin \mathcal{I}_{\text{KL}} \\ -\rho_i A_i + \beta_{\text{cov}} |\log \pi_{\theta}(y_i \mid y_{<i}) - \log \pi_{\theta_{\text{old}}}(y_i \mid y_{<i})| & \text{if } i \in \mathcal{I}_{\text{KL}} \end{cases} \quad (8)$$

The first case is the standard clipped GRPO surrogate (Eq. 1). The second case replaces clipping with a targeted penalty: the term  $|\log \pi_{\theta}(y_i \mid y_{<i}) - \log \pi_{\theta_{\text{old}}}(y_i \mid y_{<i})| = |\log \rho_i|$  is the absolute log-importance-ratio, an  $\ell_1$  surrogate for the token-level KL between  $\pi_{\theta_{\text{old}}}$  and  $\pi_{\theta}$  that mirrors the targeted KL penalty of Cui et al. [2025] while remaining symmetric in the direction of the shift;  $\beta_{\text{cov}} > 0$  controls the penalty strength.

**Total Loss:** The total batch loss, with a global KL penalty against the frozen reference policy  $\pi_{\text{ref}}$ , is:

$$\mathcal{L}(\theta) = \frac{1}{N} \sum_{i=1}^N \mathcal{L}(y_i; \theta) + \gamma D_{\text{KL}}(\pi_{\theta} \parallel \pi_{\text{ref}}) \quad (9)$$

where  $\gamma \geq 0$  is the reference KL coefficient of GRPO. Following [Cui et al., 2025], we use  $k = 0.02$ , as the  $\sim 98\%$  of tokens with normal covariance receive the standard clipped GRPO update, while the  $\sim 2\%$  of outlier tokens, those responsible for gradient concentration, receive the additional KL penalty that prevents entropy collapse. This targets only collapse-driving tokens, preserving exploration without degrading optimization for most tokens.

## 4 Experiments & Results

### 4.1 Experimental Setup

**Training details.** We use Qwen2.5-1.5B-Base and Qwen2.5-3B-Base [Yang et al., 2024] as the base models for all experiments. We use the MATH training split of MATH-lighteval [Hendrycks et al., 2021], as the source of unlabeled training prompts. All models are trained with full finetuning using GRPO [Shao et al., 2024] as the base optimizer with a learning rate of  $3 \times 10^{-6}$  and cosine scheduling. We use  $G = 7$  rollouts per prompt with a maximum completion length of 3072 tokens. The GRPO KL penalty coefficient is set to  $\gamma = 0.005$ , following [Zhao et al., 2025b]. For our method, we set equal reward-channel weights  $\alpha = \beta = 0.5$ , use a top-2% covariance threshold  $k = 0.02$ , and set  $\beta_{\text{cov}} = 0.05$ . Training is conducted on a single node with 4 NVIDIA GH200 120GB GPUs. The effective batch size is 882 prompts per gradient update, corresponding to 6,174 rollouts per step. We train for 40 epochs (340 steps) using huggingface-trl framework [von Werra et al., 2020]. The full training, optimization, batch, hardware, and evaluation hyperparameters are reported in Appendix F and Table 6.

**Evaluation.** We evaluate on seven benchmarks spanning in-distribution to out-of-distribution reasoning: GSM8K [Cobbe et al., 2021], MATH500 [Hendrycks et al., 2021], MMLU-Pro [Wang et al., 2024] (5-shot CoT), AIME 2024/2025, LiveCodeBench v6 [Jain et al., 2025] (LCB; pass@1, all-tests-must-pass), and CRUXEval-O [Gu et al., 2024] (output-prediction via ZeroEval [Lin, 2024] OEQA template). Math benchmarks are scored with math\_verify using the training chat-style prompt; MMLU-Pro uses TIGER-Lab’s canonical 5-shot CoT completion-style prompt [Wang et al., 2024]. LCB evaluation follows the lighteval [Habib et al., 2023] pipeline verbatim. Among the 5 math benchmarks, the performance on AIME 2024/2025 can be considered as OOD generalization because AIME problems require novel multi-step olympiad-level reasoning with extremely low base-rate success which does not reflect in our training dataset. The two coding tasks are also considered as OOD generalization as the methods were not trained on coding datasets.

### 4.2 Main Results

**Math-reasoning Performance.** Table 1 reports greedy ( $T=0, n=1$ ) pass@1 at a fixed step-160 (epoch 18) checkpoint across three math benchmarks for both Qwen2.5-1.5B and Qwen2.5-3B. We

Table 1: Performance on three math-reasoning benchmarks and two code-reasoning after extended training (18 epochs). Best *unsupervised* value per column in **bold**.

Model	Method	Math-reasoning			Code-reasoning	
		GSM8K	MATH500	MMLU-Pro	LCB v6	CRUXEval-O
Qwen2.5-1.5B	GRPO with ground-truth reward	74.9	55.2	31.6	1.7	24.9
	INTUITOR	22.4	22.6	24.5	0.8	12.6
	Multi-reward	<b>69.5</b>	46.0	27.7	<b>3.3</b>	<b>21.8</b>
	Multi-reward + KL-Cov	68.3	<b>51.6</b>	<b>29.9</b>	2.6	20.5
Qwen2.5-3B	GRPO with ground-truth reward	84.9	64.4	40.3	6.4	41.0
	INTUITOR	73.3	55.0	33.1	6.6	36.1
	Multi-reward	<b>82.8</b>	60.0	<b>39.3</b>	4.4	<b>41.0</b>
	Multi-reward + KL-Cov	80.7	<b>62.4</b>	39.0	<b>7.7</b>	38.3

select step 160 as a representative mid-training checkpoint, prior to the late-stage collapse dynamics observed in single-signal continued training; full trajectories are provided in Figure 2. On every math benchmark, the best unsupervised method is one of our two multi-reward variants. On 1.5B, multi-reward + KL-Cov leads INTUITOR by 45.9, 29.0, and 5.4 pp on GSM8K, MATH500, and MMLU-Pro, and trails supervised GRPO-GT by only 6.6, 3.6, and 1.7 pp. The gains are consistent across model scales: on the 3B model both variants also outperform INTUITOR and remain on par with GRPO-GT. The results on AIME 2024/2025 are reported in Appendix A.

**Code-reasoning generalization.** We evaluate code-reasoning generalization to assess whether math-trained reasoning structure transfers to code-execution domains without any code-domain training. Table 1 reports results on two coding benchmarks, LCB v6 and CRUXEval-O, evaluated at the same step-160 checkpoints. On Qwen2.5-3B, multi-reward (with or without KL-Cov) tracks supervised GRPO-GT closely: plain multi-reward matches GRPO-GT exactly on CRUXEval-O (41.0%), and multi-reward + KL-Cov is the strongest unsupervised method on LCB (7.7%, ahead of GRPO-GT at 6.4% and INTUITOR at 6.6%). On Qwen2.5-1.5B all methods sit near floor on LCB (0.8–3.3%) so the pattern is dominated by base-model capability; on CRUXEval-O the same INTUITOR-vs-multi-reward separation as the math benchmarks holds (12.6% vs. 21.8/20.5%).

**Training Dynamics: Model Collapse.** In Figure 2, we illustrate model collapse by showing the full training dynamics, with checkpoints evaluated every 20 training steps. We report results on GSM8K (in-distribution arithmetic), MATH500 (in-distribution competition math), and MMLU-Pro (OOD multiple-choice reasoning), for both Qwen2.5-1.5B and Qwen2.5-3B. Across these settings, we observe two consistent patterns at both scales. First, single-reward INTUITOR exhibits model collapse due to reward-hacking (See Appendix G): self-certainty peaks early, around steps 40–60, and then declines monotonically, reaching near-zero math accuracy. Second, multi-reward + KL-Cov remains stable across the full training trajectory. It performs on par with supervised GRPO-GT, retaining 89–93% of peak performance on 1.5B and 95–99% on 3B at step 340. We also observe that multi-reward training alone delays collapse but does not fully prevent it, especially on 1.5B.

### 4.3 Ablation Study

We isolate the contribution of each component with two trajectory-level ablations: a single-reward decomposition that targets the complementary-rewards claim, and a  $\beta_{\text{cov}}$  sweep that targets sensitivity to the KL-Cov coefficient. The component-removal table, the INTUITOR+KL-Cov trajectory, and the full  $\beta_{\text{cov}}$  tabulation are deferred to Appendix C and D.

**Single- & Multi-reward analysis without KL-Cov.** Here, we analyze the effect of single- and multi-reward structures in the absence of KL-Cov regularization by comparing three reward settings based on cluster voting, self-certainty, and their combination. All three settings are initialized from Qwen2.5-1.5B-Base and trained for 280 steps. Figure 3 reports pass@1 accuracy together with the corresponding mean completion length and entropy.

*Cluster-only* training attains the highest early GSM8K accuracy (75.0% at step 60), but collapses abruptly, with GSM8K dropping from 71.8% to 0.0% between steps 120 and 140 and MATH500 from 35.4% to 1.4%. Since entropy and completion length increase after collapse, this is not a low-entropy

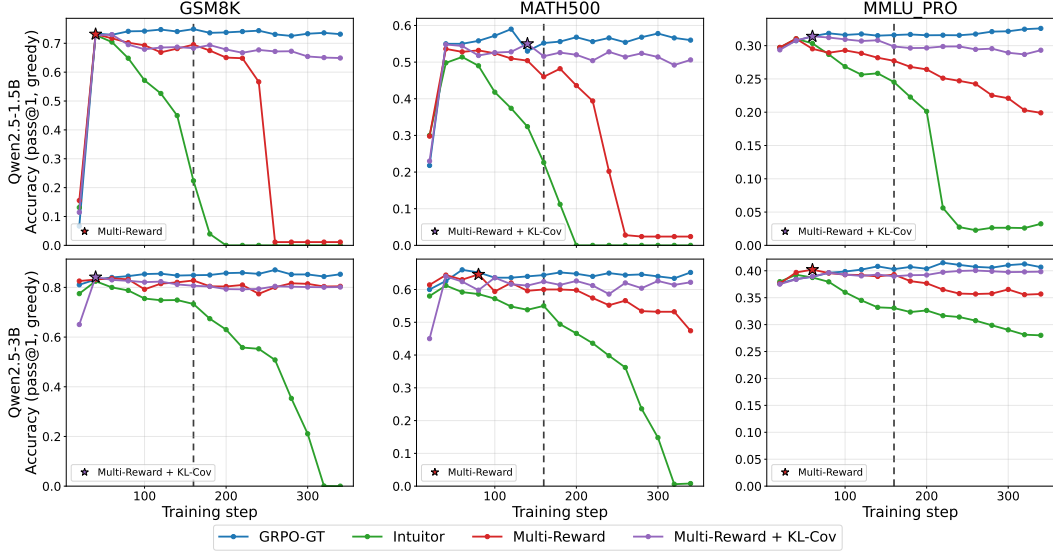


Figure 2: Accuracy (pass@1) trajectories on GSM8K, MATH500, MMLU-Pro for Qwen2.5-1.5B (top) and Qwen2.5-3B (bottom). The dashed vertical line marks step 160 (Table 1); the star (★) marks the peak among unsupervised methods (GRPO-GT excluded), labeled in-axis. Only multi-reward + KL-Cov tracks GRPO-GT through the full 340-step horizon at both scales.

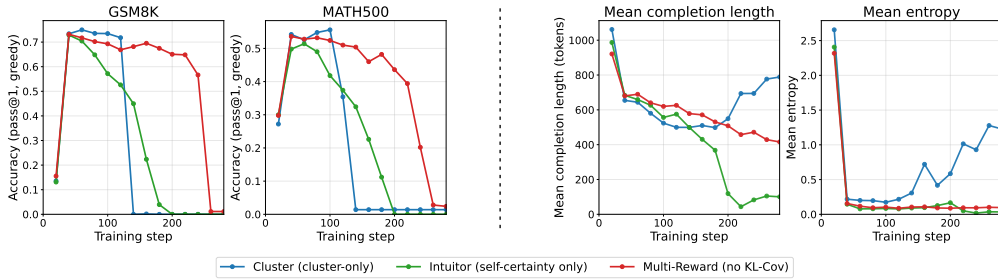


Figure 3: Single- & multi-reward analysis (no KL-Cov) on Qwen2.5-1.5B. Left: GSM8K and MATH500 pass@1. Right: training-time mean completion length and mean entropy. Cluster-only (blue) shows answer-mode collapse (rising entropy, lengthening generations); INTUITOR (green) shows token-mode collapse (entropy in  $[0.03, 0.17]$ , length crashing to  $\sim 100$  tokens); multi-reward without KL-Cov (red) blocks both exploits but eventually collapses by step 260.

short-template failure; rather, the model produces long completions whose extracted answers collapse to a dominant cluster, exploiting the answer-level reward. In contrast, *self-certainty-only* (i.e., Intuitor) training induces token-mode (or entropy) collapse: entropy falls from 2.4 to 0.08 nats by step 60, and completion length shrinks from  $\sim 990$  to  $\sim 100$  tokens. The vulnerability to answer-space drift and token-space drift remains in case of single-reward cluster-voting and self-certainty.

The *multi-reward* setting without KL-Cov is more stable than either single reward, in line with the complementary structure of the two signals. Empirically, this complementarity broadens the stable training window: GSM8K remains in the 65–73% range through step 200, and MATH500 stays above 46% through step 180. Nevertheless, the run eventually collapses, with GSM8K falling from 56.6% to 1.1% between steps 240 and 260. Thus, multi-reward training delays degeneration but does not completely prevent it, motivating the need for KL-Cov regularization.

**KL-Cov coefficient sweep.** We sweep  $\beta_{\text{cov}} \in \{0.0005, 0.05, 0.1\}$  for the full multi-reward objective. Figure 4 shows that all three settings produce tightly clustered trajectories, keeping completion length within 1000–1300 tokens and maintaining stable math accuracy through step 280. By contrast, removing KL-Cov causes collapse around step 240, with short template-like completions and math

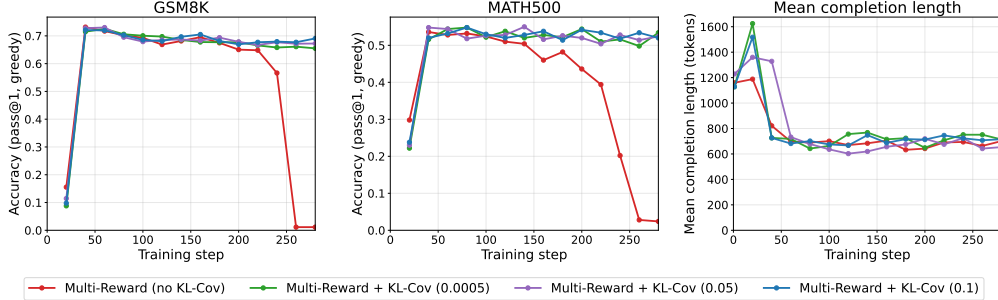


Figure 4: KL-Cov  $\beta_{\text{cov}}$  sweep on the full multi-reward objective (Qwen2.5-1.5B). All three coefficients ( $\beta_{\text{cov}} \in \{0.0005, 0.05, 0.1\}$ ) maintain stable accuracy and completion length through step 280; the no-KL-Cov baseline (red) collapses around step 240.

accuracy dropping to  $\sim 1\text{--}2\%$ . Additional results are provided in Table 5 in Appendix D. Overall, KL-Cov behaves as a robust stabilizer rather than a highly sensitive regularizer, and our default value  $\beta_{\text{cov}} = 0.05$  does not require per-model retuning.

## 5 Discussion

Figure 3 suggests that cluster voting and self-certainty expose complementary reward-hacking directions. The cluster-voting reward depends only on the extracted answer and is invariant to the token-level reasoning path. As a result, the policy can exploit this objective by drifting in reasoning space while concentrating final answers into a dominant cluster, producing long, high-entropy completions after collapse. Conversely, self-certainty acts directly on token probabilities but is invariant to answer correctness, allowing the policy to exploit the reward by becoming confidently deterministic, yielding short template-like outputs. The multi-reward objective partially mitigates these failures because each reward constrains a direction left under specified by the other. Cluster voting discourages arbitrary confident templates that do not produce consistent answers, while self-certainty constrains unconstrained token-level drift under cluster voting. Empirically, this widens the stable training window and yields more controlled entropy and length dynamics, avoiding both the entropy rebound of cluster-only and the premature entropy collapse of self-certainty-only training.

Multi-objective reward design is motivated by the idea that individual signals capture distinct but incomplete aspects of desired behavior and can be additively combined [Zhao et al., 2025b]. Our work provides the first empirical demonstration of this effect in reasoning-training. However, though multi-reward training closes off single-reward loopholes, complementarity alone is insufficient and KL-Cov remains necessary to stabilize the residual optimization dynamics.

**Limitations.** Our framework introduces additional hyperparameters beyond standard GRPO, including the top- $k$  covariance fraction  $\beta_{\text{cov}}$  and the channel weights  $\alpha$  and  $\beta$ . The KL-Cov sweep in Figure 4 suggests that performance is largely insensitive to  $\beta_{\text{cov}}$  across a  $200\times$  range. However, we do not conduct a systematic study of the relative weighting  $\alpha/\beta$  and instead adopt the symmetric default  $\alpha = \beta = 0.5$  throughout. In addition, the method relies on a sufficiently capable base model: the pretrained model’s initial reasoning ability plays an important role in its success. The proposed framework does not include safeguards for models with poor initial reasoning capability.

## 6 Conclusion

This paper presents a multi-reward framework with KL-Cov regularization for reinforcement learning from internal feedback (RLIF) mechanism in large language models. In response to the collapse observed under single-reward training, our approach combines two complementary intrinsic signals. Together, these rewards provide a richer training signal that mitigates the distinct degeneracies induced by either reward alone. KL-Cov further stabilizes optimization by targeting the small subset of tokens responsible for disproportionate entropy reduction, preventing late-stage collapse while preserving stable reasoning.

Across mathematical reasoning and coding benchmarks, our method achieves performance close to supervised RLVR approaches such as GRPO, without requiring gold-standard solutions. These results highlight the potential of multi-reward RLIF as a scalable alternative to externally supervised reinforcement learning. More broadly, they suggest that future work can explore additional internal signals, potentially stronger than those studied here, to support stable long-horizon reasoning. Such stability is central to RLIF: as models scale and reasoning trajectories become more complex, training must preserve exploration beyond early high-confidence behaviors rather than collapse into narrow reward-seeking patterns.

**Acknowledgment:** This work was supported as part of the “Swiss AI initiative” by a grant from the Swiss National Supercomputing Centre (CSCS) under project ID a168 on Alps.

## References

- Shivam Agarwal, Zimin Zhang, Lifan Yuan, Jiawei Han, and Hao Peng. The unreasonable effectiveness of entropy minimization in LLM reasoning. *arXiv preprint arXiv:2505.15134*, 2025.
- Peter Chen, Xiaopeng Li, Ziniu Li, Wotao Yin, Xi Chen, and Tianyi Lin. Exploration vs exploitation: Rethinking RLVR through clipping, entropy, and spurious reward. In *International Conference on Learning Representations (ICLR)*, 2026. URL <https://arxiv.org/abs/2512.16912>.
- Karl Cobbe, Vineet Kosaraju, Mohammad Bavarian, Mark Chen, Heewoo Jun, Lukasz Kaiser, Matthias Plappert, Jerry Tworek, Jacob Hilton, Reiichiro Nakano, Christopher Hesse, and John Schulman. Training verifiers to solve math word problems. *arXiv preprint arXiv:2110.14168*, 2021.
- Ganqu Cui, Yuchen Zhang, Jiacheng Chen, Lifan Yuan, Zhi Wang, Yuxin Zuo, Haozhan Li, Yuchen Fan, Huayu Chen, Weize Chen, Zhiyuan Liu, Hao Peng, Lei Bai, Wanli Ouyang, Yu Cheng, Bowen Zhou, and Ning Ding. The entropy mechanism of reinforcement learning for reasoning language models. *arXiv preprint arXiv:2505.22617*, 2025.
- DeepSeek-AI. DeepSeek-R1: Incentivizing reasoning capability in LLMs via reinforcement learning. *arXiv preprint arXiv:2501.12948*, 2025.
- Leo Gao, John Schulman, and Jacob Hilton. Scaling laws for reward model overoptimization, 2022. URL <https://arxiv.org/abs/2210.10760>.
- Alex Gu, Baptiste Rozière, Hugh Leather, Armando Solar-Lezama, Gabriel Synnaeve, and Sida Wang. CRUXEval: A benchmark for code reasoning, understanding and execution. In *International Conference on Machine Learning (ICML)*, 2024. URL <https://arxiv.org/abs/2401.03065>.
- Nathan Habib, Clémentine Fourrier, Hynek Kydlíček, Thomas Wolf, and Lewis Tunstall. Lighteval: A lightweight framework for LLM evaluation. <https://github.com/huggingface/lighteval>, 2023.
- Bingxiang He, Yuxin Zuo, Zeyuan Liu, Shangziqi Zhao, Zixuan Fu, Junlin Yang, Cheng Qian, Kaiyan Zhang, Yuchen Fan, Ganqu Cui, Xiusi Chen, Youbang Sun, Xingtai Lv, Xuekai Zhu, Li Sheng, Ran Li, Huan-ang Gao, Yuchen Zhang, Bowen Zhou, Zhiyuan Liu, and Ning Ding. How far can unsupervised RLVR scale LLM training? In *International Conference on Learning Representations (ICLR)*, 2026. URL <https://arxiv.org/abs/2603.08660>.
- Dan Hendrycks, Collin Burns, Saurav Kadavath, Akul Arora, Steven Basart, Eric Tang, Dawn Song, and Jacob Steinhardt. Measuring mathematical problem solving with the math dataset. *arXiv preprint arXiv:2103.03874*, 2021.
- Chengsong Huang, Wenhao Yu, Xiaoyang Wang, Hongming Zhang, Zongxia Li, Ruosen Li, Jiabin Huang, Haitao Mi, and Dong Yu. R-Zero: Self-evolving reasoning LLM from zero data. *arXiv preprint arXiv:2508.05004*, 2025.
- Naman Jain, King Han, Alex Gu, Wen-Ding Li, Fanjia Yan, Tianjun Zhang, Sida Wang, Armando Solar-Lezama, Koushik Sen, and Ion Stoica. LiveCodeBench: Holistic and contamination free evaluation of large language models for code. In *International Conference on Learning Representations (ICLR)*, 2025. URL <https://arxiv.org/abs/2403.07974>.

- Lorenz Kuhn, Yarin Gal, and Sebastian Farquhar. Semantic uncertainty: Linguistic invariances for uncertainty estimation in natural language generation. In *International Conference on Learning Representations (ICLR)*, 2023.
- Yuchen Lin. ZeroEval: A unified framework for evaluating language models. <https://github.com/yuchenlin/ZeroEval>, 2024.
- Shih-Yang Liu, Xin Dong, Ximing Lu, Shizhe Diao, Peter Belcak, Mingjie Liu, Min-Hung Chen, Hongxu Yin, Yu-Chiang Frank Wang, Kwang-Ting Cheng, Yejin Choi, Jan Kautz, and Pavlo Molchanov. GDPO: Group reward-decoupled normalization policy optimization for multi-reward RL optimization. *arXiv preprint arXiv:2601.05242*, 2026.
- Mihir Prabhudesai, Lili Chen, Alex Ippoliti, Katerina Fragkiadaki, Hao Liu, and Deepak Pathak. Maximizing confidence alone improves reasoning. *arXiv preprint arXiv:2505.22660*, 2025.
- Sheikh Shafayat, Fahim Tajwar, Ruslan Salakhutdinov, Jeff Schneider, and Andrea Zanette. Can large reasoning models self-train? *arXiv preprint arXiv:2505.21444*, 2025.
- Zhihong Shao, Peiyi Wang, Qihao Zhu, Runxin Xu, Junxiao Song, Mingchuan Zhang, Y. K. Li, Y. Wu, and Daya Guo. DeepSeekMath: Pushing the limits of mathematical reasoning in open language models. *arXiv preprint arXiv:2402.03300*, 2024.
- Leandro von Werra, Younes Belkada, Lewis Tunstall, Edward Beeching, Tristan Thrush, Nathan Lambert, Shengyi Huang, Kashif Rasul, and Quentin Gallouédec. TRL: Transformers Reinforcement Learning, 2020. URL <https://github.com/huggingface/trl>.
- Yubo Wang, Xueguang Ma, Ge Zhang, Yuansheng Ni, Abhranil Chandra, Shiguang Guo, Weiming Ren, Aaran Arulraj, Xuan He, Ziyang Jiang, Tianle Li, Max Ku, Kai Wang, Alex Zhuang, Rongqi Fan, Xiang Yue, and Wenhui Chen. MMLU-Pro: A more robust and challenging multi-task language understanding benchmark. In *Advances in Neural Information Processing Systems (NeurIPS)*, 2024.
- Xiaomi LLM-Core Team. MiMo: Unlocking the reasoning potential of language model – from pretraining to posttraining. *arXiv preprint arXiv:2505.07608*, 2025.
- An Yang, Baosong Yang, Beichen Zhang, Binyuan Hui, Bo Zheng, Bowen Yu, Chengyuan Li, Dayiheng Liu, Fei Huang, Haoran Wei, et al. Qwen2.5 technical report. *arXiv preprint arXiv:2412.15115*, 2024.
- Wenjie Yang, Mao Zheng, Mingyang Song, Zheng Li, and Sitong Wang. SSR-Zero: Simple self-rewarding reinforcement learning for machine translation. *arXiv preprint arXiv:2505.16637*, 2025.
- Qiang Zhang, Hao Wu, Changsheng Zhang, Peilin Zhao, and Yatao Bian. Right question is already half the answer: Fully unsupervised LLM reasoning incentivization. *arXiv preprint arXiv:2504.05812*, 2025a.
- Yanzhi Zhang, Zhaoxi Zhang, Haoxiang Guan, Yilin Cheng, Yitong Duan, Chen Wang, Yue Wang, Shuxin Zheng, and Jiyan He. No free lunch: Rethinking internal feedback for LLM reasoning. *arXiv preprint arXiv:2506.17219*, 2025b.
- Zizhuo Zhang, Jianing Zhu, Xinmu Ge, Zihua Zhao, Zhanke Zhou, Xuan Li, Xiao Feng, Jiangchao Yao, and Bo Han. Co-rewarding: Stable self-supervised RL for eliciting reasoning in large language models. *arXiv preprint arXiv:2508.00410*, 2025c.
- Andrew Zhao, Yiran Wu, Yang Yue, Tong Wu, Quentin Xu, Matthieu Lin, Shenzhi Wang, Qingyun Wu, Zilong Zheng, and Gao Huang. Absolute zero: Reinforced self-play reasoning with zero data. In *Advances in Neural Information Processing Systems (NeurIPS)*, 2025a.
- Xuandong Zhao, Zhewei Kang, Aosong Feng, Sergey Levine, and Dawn Song. Learning to reason without external rewards. *arXiv preprint arXiv:2505.19590*, 2025b.
- Xiangxin Zhou, Zichen Liu, Anya Sims, Haonan Wang, Tianyu Pang, Chongxuan Li, Liang Wang, Min Lin, and Chao Du. Reinforcing general reasoning without verifiers. *arXiv preprint arXiv:2505.21493*, 2025.

Yuxin Zuo, Kaiyan Zhang, Li Sheng, Shang Qu, Ganqu Cui, Xuekai Zhu, Haozhan Li, Yuchen Zhang, Xinwei Long, Ermo Hua, Biqing Qi, Youbang Sun, Zhiyuan Ma, Lifan Yuan, Ning Ding, and Bowen Zhou. TTRL: Test-time reinforcement learning. *arXiv preprint arXiv:2504.16084*, 2025.

## A Performance on AIME

AIME 2024/2025 are at the 30-problem noise floor at the 1.5B scale (one problem  $\approx 3.3$  pp), so 1.5B numbers should be read as near-zero indicators only. On 3B, multi-reward (without KL-Cov) ties supervised GRPO-GT and INTUITOR (6.7% on AIME 2024, 3.3% on AIME 2025), while multi-reward + KL-Cov drops to 3.3% / 0.0%.

Table 2: Pass@1 (% , greedy) on AIME 2024 and AIME 2025 at the step-160 checkpoint (18 epochs). Best *unsupervised* value per column in **bold** (ties bolded together).

Model	Method	AIME 2024	AIME 2025
Qwen2.5-1.5B	GRPO with ground-truth reward	0.0	3.3
	INTUITOR	0.0	0.0
	Multi-reward	0.0	0.0
	Multi-reward + KL-Cov $\beta_{cov}=0.05$	0.0	0.0
Qwen2.5-3B	GRPO with ground-truth reward	6.7	3.3
	INTUITOR	<b>6.7</b>	<b>3.3</b>
	Multi-reward	<b>6.7</b>	<b>3.3</b>
	Multi-reward + KL-Cov $\beta_{cov}=0.05$	3.3	0.0

## B Detailed stability analysis

This appendix accompanies Figure 2 (Section 4.2) with the per-method numerical breakdown referenced in the main text. Table 3 reports peak accuracy, peak step, collapse step, end-of-horizon accuracy, and retention for both Qwen2.5-1.5B and Qwen2.5-3B. Three observations follow from the figure together with this table; the AIME 2024/2025 far-OOD probe is reported separately in Appendix A.

Table 3: **Stability under continued training** (greedy pass@1) for Qwen2.5-1.5B and Qwen2.5-3B. Each cell reports the metric on three benchmarks as GSM8K / MATH500 / MMLU-Pro. *Peak (%)* is the best pass@1 reached during the trajectory, and *Peak step* is the first checkpoint at which that peak is reached. *Collapse step* is the first checkpoint *after peak* at which accuracy drops below 50% of peak (“—” if never crossed by step 340). *Step-340* is end-of-horizon accuracy and *Retention* is step-340/peak.

Model	Method	Peak (%)	Peak step	Collapse step	Step-340 (%)	Retention (%)
		GSM8K/M500/MMLU	GSM8K/M500/MMLU	GSM8K/M500/MMLU	GSM8K/M500/MMLU	GSM8K/M500/MMLU
Qwen2.5-1.5B	GRPO with ground-truth reward	74.9/59.0/32.6	160/120/340	—/—/—	73.2/56.0/32.6	97.7/94.9/100.0
	INTUITOR	72.9/51.4/31.0	40/60/40	160/160/220	0.0/0.0/3.2	0.0/0.0/10.4
	Multi-reward	<b>73.2</b> /53.6/31.0	40/40/40	260/240/—	1.1/2.4/19.9	1.6/4.5/64.2
	Multi-reward + KL-Cov $\beta_{cov}=0.05$	73.0/ <b>55.0</b> / <b>31.4</b>	60/140/60	—/—/—	<b>64.9</b> / <b>50.6</b> / <b>29.3</b>	88.9/92.0/93.3
Qwen2.5-3B	GRPO with ground-truth reward	87.0/66.0/41.5	260/60/220	—/—/—	85.3/65.2/40.7	98.0/98.8/98.0
	INTUITOR	82.5/61.2/39.3	40/40/40	280/280/—	0.0/0.8/28.0	0.0/1.3/71.4
	Multi-reward	83.6/ <b>64.6</b> / <b>40.2</b>	60/80/60	—/—/—	80.4/47.4/35.7	96.2/73.4/88.7
	Multi-reward + KL-Cov $\beta_{cov}=0.05$	<b>84.2</b> /64.0/40.0	40/40/260	—/—/—	80.1/ <b>62.2</b> / <b>39.8</b>	95.2/97.2/99.5

**Three observations from Figure 2 and Table 3.** (1) **Single-signal methods collapse catastrophically.** INTUITOR peaks at step 40 with 72.9% pass@1 and then declines monotonically: 64.8% (step 80)  $\rightarrow$  44.9% (step 140)  $\rightarrow$  22.4% (step 160)  $\rightarrow$  0% from step 200 onward. By the end of training the policy produces no parseable answers on GSM8K. This matches the theoretical prediction of Zhang et al. [2025b], He et al. [2026], Shafayat et al. [2025]: an objective that depends on a single reward signal can be maximized by degenerate policies that emit the same high-confidence (but content-free) template regardless of input.

(2) **Multi-reward without KL-Cov delays collapse on 1.5B but is not consistently stable.** Plain multi-reward (cluster voting + self-certainty, no KL-Cov) reaches a competitive early peak of 73.2%

(step 40) on GSM8K and 53.6% (step 40) on MATH500, and holds this level for considerably longer than either single-signal method: GSM8K stays in the 65–73% band through step 200 (and above 56% through step 240), while MATH500 stays above 46% through step 180. Around step 240 it enters a rapid degeneration phase—GSM8K drops from 56.6% at step 240 to 1.1% at step 260—and the policy collapses to 1.1% / 2.4% on GSM8K / MATH500 by step 260, staying there through step 340. The complementary reward structure (cluster voting and self-certainty, with complementary policy gradients per) thus *slows* convergence to the degenerate fixed point, extending the usable training window by  $\approx 60$  steps versus INTUITOR, but does not, by itself, prevent collapse.

**(3) Multi-reward + KL-Cov is the only unsupervised configuration that remains robust across both scales.** Multi-reward + KL-Cov ( $\beta=0.05$ ) peaks at 73.0% GSM8K (step 60) and 55.0% MATH500 (step 140) on 1.5B, then remains in the 64.9–73.0% band on GSM8K and 49.2–55.0% band on MATH500 through step 340. On 3B it is even more stable, retaining 95.2% / 97.2% / 99.5% of peak on GSM8K / MATH500 / MMLU-Pro. The trajectories closely track supervised GRPO-GT, supporting the claim that KL-Cov is the ingredient that prevents residual gradient concentration on outlier tokens that plain multi-reward alone cannot suppress.

## C Component ablation

Table 4 reports the component-removal ablation summarized in Section 4.3. Peaks differ by less than 2 points across configurations; the diagnostic difference is at step 340, where every reduced configuration collapses on math while the full method retains  $\geq 50\%$ .

Table 4: Component ablation on Qwen2.5-1.5B (**peak/step-340** pass@1, %). Peaks are tight; step-340 is the diagnostic. <sup>†</sup>Cluster-only was trained to step 280; math accuracy has been flat at the reported value since step 140 (Figure 3).

Configuration	GSM8K	MATH500
	peak / step-340	peak / step-340
Full model (all components)	<b>73.0 / 64.9</b>	<b>55.0 / 50.6</b>
w/o KL-Cov (multi-reward only)	73.2 / 1.1	53.6 / 2.4
w/o cluster voting (self-certainty only $\equiv$ INTUITOR)	72.9 / 0.0	51.4 / 0.0
w/o self-certainty (cluster voting only)	75.0 / 0.0 <sup>†</sup>	55.6 / 1.4 <sup>†</sup>

## D Detailed KL-Cov $\beta_{\text{cov}}$ sweep and KL-Cov on single-signal INTUITOR

This appendix accompanies Figure 4 (Section 4.3) with the per-method numerical breakdown and the complementary INTUITOR+KL-Cov ablation referenced in the main text.

**Numerical breakdown of the  $\beta_{\text{cov}}$  sweep.** On the multi-reward base, peaks fall in a narrow 72.1–73.0% band on GSM8K and 54.8–55.0% on MATH500; step-160 accuracy lies within 67.8–70.5% on GSM8K and 51.6–53.8% on MATH500— $\sim 2.7$  percentage points of step-160 spread across a  $200\times$  range of  $\beta_{\text{cov}}$  (Table 5).

**KL-Cov on single-signal INTUITOR.** Does KL-Cov alone—on top of a single-signal reward—suffice to prevent collapse? It does not (Figure 5). Adding KL-Cov ( $\beta_{\text{cov}}=0.02$ ) to vanilla INTUITOR leaves peaks essentially unchanged (72.6 vs. 72.9 on GSM8K, 51.2 vs. 51.4 on MATH500) but doubles step-160 retention (46.2% / 38.2% vs. 22.4% / 22.6%). Past step 200, however, the policy still crashes to  $<1\%$  on both benchmarks: on a single-signal reward the degenerate fixed point is too strong an attractor for KL-Cov alone to escape. The mean-completion-length panel shows the mechanism—KL-Cov delays the collapse into the short template-like regime, but does not prevent the eventual fall.

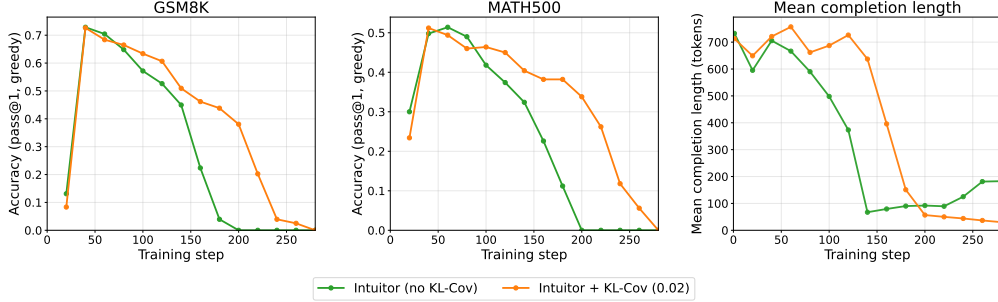


Figure 5: INTUITOR + KL-Cov ablation on Qwen2.5-1.5B (steps 0–280). KL-Cov ( $\beta_{\text{cov}}=0.02$ ) doubles step-160 accuracy versus vanilla INTUITOR but does not prevent collapse past step 200.

Table 5: KL-Cov sweep merged across the INTUITOR (single-signal) and multi-reward base methods on Qwen2.5-1.5B, reporting **peak / step-160** pass@1 (%). The peak captures best-case accuracy; the step-160 column reflects mid-horizon stability under continued training. Within each base reward (top: INTUITOR sweep; bottom: multi-reward sweep), KL-Cov is the only variable. Bold marks the chosen full-method configuration. *Top block*: KL-Cov on single-signal INTUITOR roughly doubles step-160 retention on math benchmarks (e.g., GSM8K 22.4  $\rightarrow$  46.2%) but cannot keep pace with the complementary reward structure of multi-reward, and on a longer horizon ( $\geq 200$  steps) eventually collapses too. *Bottom block*: KL-Cov is remarkably insensitive to  $\beta_{\text{cov}}$ —a 200 $\times$  range produces only  $\sim 2.7$  pp of step-160 spread.

Configuration	GSM8K peak / step-160	MATH500 peak / step-160	MMLU-Pro peak / step-160
<i>Single-signal reward (INTUITOR)</i>			
INTUITOR (no KL-Cov)	72.9 / 22.4	51.4 / 22.6	31.0 / 24.5
INTUITOR + KL-Cov ( $\beta_{\text{cov}}=0.02$ )	72.6 / <b>46.2</b>	51.2 / <b>38.2</b>	30.9 / <b>24.9</b>
<i>Multi-reward (cluster voting + self-certainty + GDPO)</i>			
Multi-reward (no KL-Cov)	73.2 / 69.5	53.6 / 46.0	31.0 / 27.7
Multi-reward + KL-Cov ( $\beta_{\text{cov}}=0.0005$ )	72.6 / 67.8	54.8 / 52.8	31.6 / 30.7
Multi-reward + KL-Cov ( $\beta_{\text{cov}}=0.05$ ) (chosen)	<b>73.0</b> / 68.3	<b>55.0</b> / 51.6	31.4 / 29.9
Multi-reward + KL-Cov ( $\beta_{\text{cov}}=0.1$ )	72.1 / <b>70.5</b>	54.8 / <b>53.8</b>	<b>31.8</b> / <b>30.4</b>

## E Per-channel GDPO normalization vs. naïve combination

This appendix isolates the contribution of per-channel GDPO normalization in the multi-reward advantage of Eq. 4–5. We compare two policy-update variants on Qwen2.5-1.5B with the multi-reward + KL-Cov ( $\beta_{\text{cov}}=0.05$ ) objective; everything except the advantage construction is held fixed (same prompts, rollouts, KL-Cov regularizer, optimizer, and seeds).

**Variants.** Let  $R_g^{(\text{cf})}$  denote the (cluster+format) channel and  $R_g^{(\text{sc})}$  the self-certainty channel for rollout  $g$  in a  $G$ -sample group, and let  $\hat{z}(\cdot)$  denote per-group  $z$ -score normalization.

- *Per-channel GDPO norm (ours)*. Each channel is  $z$ -scored *within its own group* before being combined:  $A_g = w_{\text{cf}} \hat{z}(R^{(\text{cf})})_g + w_{\text{sc}} \hat{z}(R^{(\text{sc})})_g$ .
- *Combine-then-normalize*. Raw weighted rewards are summed at their native scales *first*, and a single  $z$ -score is applied to the combined signal:  $A_g = \hat{z}(w_{\text{cf}} R^{(\text{cf})} + w_{\text{sc}} R^{(\text{sc})})_g$ .

Both variants feed the policy update an advantage with  $\text{std} \approx 1$ , so any difference is attributable to the order of normalization, not to the magnitude of the gradient.

**Result (downstream accuracy).** Per-channel normalization holds its peak through training, while the naïve combination peaks early and drifts down (Figure 6). The gap is sharpest on GSM8K—peak 73.0% (per-channel) vs. 69.4% (combine-then-normalize), step-280 67.2% vs. 46.5%—and consistent on MATH500 and MMLU-Pro. Mechanistically, when the two channels are summed at

their native scales before normalization, the higher-variance channel dominates the combined signal: the single  $z$ -score then implicitly down-weights the lower-variance channel by exactly the ratio of pre-normalization standard deviations. Per-channel  $z$ -scoring removes this implicit re-weighting and lets  $w_{cf}$ ,  $w_{sc}$  control the channel mix as intended.

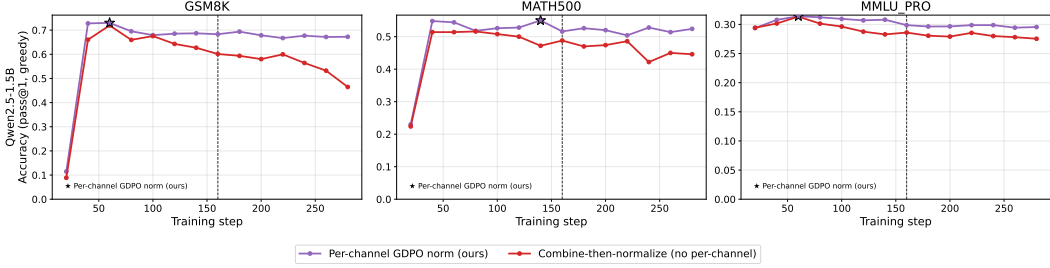


Figure 6: GDPO-normalization ablation on Qwen2.5-1.5B with the full multi-reward + KL-Cov ( $\beta_{cov}=0.05$ ) objective. Replacing per-channel  $z$ -score with a single combine-then-normalize step degrades GSM8K substantially and MATH500 / MMLU-Pro consistently across the entire trajectory; the gap widens past step 160 (vertical line). Stars mark the overall peak per benchmark.

**Gradient-space diagnosis.** To confirm that the trajectory gap in Figure 6 is driven by the variance-weighted channel collapse predicted above, and not by an unrelated optimization artifact, we instrument training with a lightweight magnitude probe in per-token logprob space. The choice of logprob space rather than parameter space can be argued by the chain rule: any loss that depends on the policy only through its per-token logprobs  $\ell$  has parameter gradient  $\nabla_{\theta} \mathcal{L} = J^{\top} \nabla_{\ell} \mathcal{L}$ , where the Jacobian  $J = \partial \ell / \partial \theta$  depends only on the model and not on which reward channel produced  $\mathcal{L}$ . The same  $J^{\top}$  multiplies both channel gradients at every step, so a  $k \times$  gap at logprob space passes through to an approximately  $k \times$  gap at parameter space (up to anisotropy of  $J^{\top}$  in the specific directions  $\nabla_{\ell} \mathcal{L}_{cf}^{lin}$  and  $\nabla_{\ell} \mathcal{L}_{sc}^{lin}$  point, which is shared across channels and therefore symmetric in the cf/sc ratio). The logprob-space norm ratio is consequently a faithful proxy for the relative magnitude with which each channel drives the parameter update, computable in  $\mathcal{O}(B \cdot S)$  without any traversal of the model and trivially safe under FSDP.

**Linearization and per-channel decomposition.** At every training step we linearize the clipped surrogate around its actual per-token coefficient  $c_{g,t}^{eff} \in \{\rho_{g,t}, \bar{\rho}_{g,t}\}$ —the unclipped ratio for unclipped or KL-Cov-gated tokens, the clipped ratio otherwise. Because both channels share the same  $c_{g,t}^{eff}$  and the same completion mask  $m_{g,t}$ , the surrogate splits cleanly into per-channel pieces

$$\mathcal{L}_{cf}^{lin} = \mathbb{E}_{g,t} \left[ -c_{g,t}^{eff} \hat{R}_{cf}(g) m_{g,t} \right], \quad \mathcal{L}_{sc}^{lin} = \mathbb{E}_{g,t} \left[ -c_{g,t}^{eff} \hat{R}_{sc}(g) m_{g,t} \right],$$

which sum to  $\mathcal{L}_{policy}^{clip} = w_{cf} \mathcal{L}_{cf}^{lin} + w_{sc} \mathcal{L}_{sc}^{lin}$  exactly the operating point (the global KL term and the KL-Cov  $|\log \rho|$  penalty do not split by channel and are excluded). We back-propagate each piece only as far as  $\ell$  and report the masked, completion-token L2 norms  $\|\nabla_{\ell} \mathcal{L}_{cf}^{lin}\|_2$  and  $\|\nabla_{\ell} \mathcal{L}_{sc}^{lin}\|_2$  at every step.

**Result.** Figure 7 shows the two channels’ logprob-space gradient norms across training under both normalization variants. Under combine-then-normalize (red),  $\|\nabla_{\ell} \mathcal{L}_{sc}^{lin}\|$  sits 10–20 $\times$  above  $\|\nabla_{\ell} \mathcal{L}_{cf}^{lin}\|$  throughout training; equivalently, the cf channel is delivering a parameter update an order of magnitude weaker than sc at every step. Under per-channel GDPO (purple) the two norms sit on the same order of magnitude, with cf in fact slightly above sc. This is the variance-weighted channel collapse predicted analytically: when raw rewards are summed before normalization, the single combined  $z$ -score implicitly down-weights the lower-variance channel by exactly the ratio  $\sigma_{cf}/\sigma_{sc}$  of pre-normalization standard deviations, and the gradient the policy actually receives from cf is suppressed by that same factor. Per-channel  $z$ -scoring removes this implicit re-weighting at the source, restoring both channels to the relative influence specified by  $w_{cf}$  and  $w_{sc}$ . The trajectory degradation in Figure 6 is therefore the predictable downstream consequence of letting one channel’s pre-normalization variance silently dictate the channel mix.

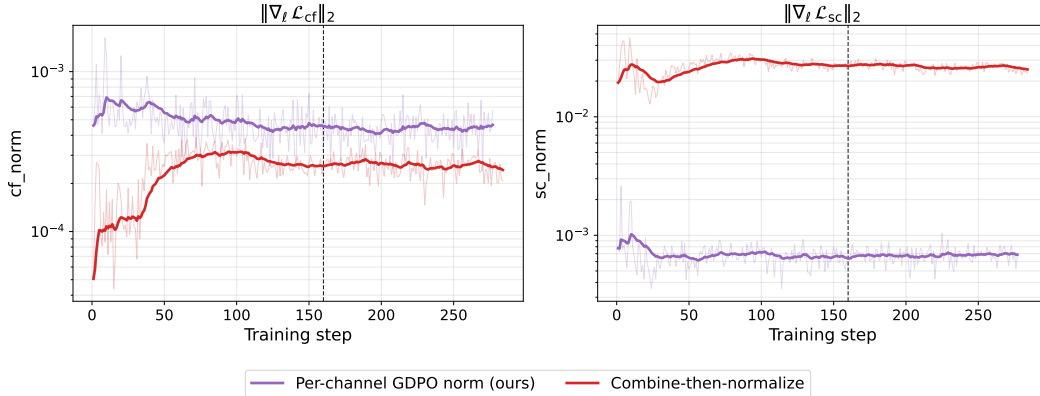


Figure 7: Logprob-space gradient norms per reward channel under each normalization variant. **Left:** cluster+format channel norm. Under combine-then-normalize (red) the cf channel is roughly an order of magnitude weaker than under per-channel GDPO (purple); the channel is being effectively silenced by the naïve combination. **Right:** self-certainty channel norm. Combine-then-normalize is 10–20 $\times$  larger, i.e. the higher-variance channel dominates the policy update by precisely the ratio of pre-normalization standard deviations. Both panels use a logarithmic  $y$ -axis. Vertical dashed line at step 160 matches Figure 6.

## F Hyperparameters

Table 6 reports the full set of training and evaluation hyperparameters. The same configuration is used across all unsupervised configurations and the GRPO-GT supervised baseline; only the reward composition,  $\beta_{\text{cov}}$  (KL-Cov coefficient), and the per-device batch / gradient-accumulation pair (smaller per-device batch on 3B for memory, with grad-accum increased to keep the effective batch fixed) vary across runs. For the  $\beta_{\text{cov}}$  sweep (Appendix D) we use  $\beta_{\text{cov}} \in \{0.0005, 0.05, 0.1\}$  on the multi-reward objective; the INTUITOR+KL-Cov ablation uses  $\beta_{\text{cov}}=0.02$ .

## G Qualitative completions: INTUITOR vs. multi-reward on GSM8K (step 240)

To make the late-horizon collapse concrete, we sample five GSM8K problems at the step-240 checkpoint of Qwen2.5-1.5B, where INTUITOR has fully collapsed (GSM8K pass@1 = 0.0%, mean completion length 282 chars) while multi-reward is still functional (pass@1 = 56.6%, mean length 1,260 chars). At this step there are 747 problems on which INTUITOR is wrong and multi-reward is correct (56.6% of the test set); the five problems below have the shortest INTUITOR completions among these. Both INTUITOR and multi-reward completions are reproduced *verbatim* from the saved evaluation logs: Markdown bold/headers are rendered as bold paragraph markers, and the model’s LaTeX-style math ( $\backslash(\dots\backslash)$ ,  $\backslash[\dots\backslash]$ ,  $\backslashboxed{\dots}$ ) is typeset as written. The same self-repeating header—“*Let’s break it down step-by-step ... Step 1: Determine X. Let’s proceed step-by-step. Step 1: Determine X.*”—recurs across all five problems (and across most of the dataset); INTUITOR has converged onto a deterministic short template that never emits a final answer.

### G.1 Problem gsm8k-499 (gold: 10)

**Question.** Mark is trying to choose between two venues for a surprise party for his wife. The first venue charges a flat fee of \$200, regardless of how many guests attend. While the second charges, \$25 per person who attends. However, the first venue does not include food, which Mark estimates will cost \$5 for each person who attends. At the second venue, food for each guest is already included in the price. How many guests are necessary for the two venues to be equal in cost?

Table 6: Training, optimization, and evaluation hyperparameters used across all configurations. Values are shared between Qwen2.5-1.5B and Qwen2.5-3B unless explicitly listed per-model. The format-reward weight applies only to the multi-reward configurations that include the boxed-format auxiliary; KL-Cov entries apply only when KL-Cov is on.

Hyperparameter	Qwen2.5-1.5B	Qwen2.5-3B
<i>Optimization</i>		
Base optimizer	AdamW	AdamW
Learning rate	$3 \times 10^{-6}$	$3 \times 10^{-6}$
LR schedule	cosine	cosine
Warmup ratio	0.1	0.1
Max gradient norm	1.0	1.0
<i>GRPO objective</i>		
Rollouts per prompt $G$	7	7
Sampling temperature (training)	1.0	1.0
Max completion length	3072	3072
PPO clip $\epsilon$	0.2	0.2
Reference-KL coefficient $\gamma$	0.005	0.005
<i>Multi-reward and KL-Cov (ours)</i>		
Cluster-reward weight $\alpha$	0.5	0.5
Self-certainty weight $\beta$	0.5	0.5
Format-reward weight	0.1	0.1
KL-Cov coefficient $\beta_{\text{cov}}$	0.05	0.05
KL-Cov top- $k$ fraction	0.02	0.02
<i>Batch and schedule</i>		
Per-device train batch	21	14
Gradient accumulation steps	14	21
Trainer GPUs (ZeRO-3)	3	3
Effective batch (prompts/step)	882	882
Rollouts per gradient step	6,174	6,174
Trained / evaluated horizon	340 steps (40 epochs)	340 steps (40 epochs)
Checkpoint interval	20 steps	20 steps
<i>Hardware (per node)</i>		
GPUs	4 × NVIDIA GH200 120GB	4 × NVIDIA GH200 120GB
Rollout server	GPU 0 (vLLM)	GPU 0 (vLLM)
Trainer	GPUs 1–3 (DeepSpeed ZeRO-3)	GPUs 1–3 (DeepSpeed ZeRO-3)
<i>Evaluation</i>		
Decoding	greedy ( $T=0, n=1$ )	greedy ( $T=0, n=1$ )
Math scorer	math_verify	math_verify
MMLU-Pro prompt	TIGER-Lab 5-shot CoT	TIGER-Lab 5-shot CoT
LCB v6 scorer	lighteval (all-tests-pass)	lighteval (all-tests-pass)
CRUXEval-O prompt	ZeroEval OEQA	ZeroEval OEQA

INTUITOR (wrong)	Multi-Reward (correct, 10)
<p>To solve this problem, we need to follow a systematic approach. Let's break it down step-by-step:</p> <p><b>Step 1: Define variables for the number of guests.</b></p> <p>Let <math>x</math> be the number of guests.</p>	<p>To determine the number of guests necessary for the two venues to be equal in cost, we need to set up equations for the total cost of each venue and then solve for the number of guests.</p> <p>Let's denote the number of guests by <math>x</math>.</p> <p>The cost of the first venue is given by:</p> $\text{Cost}_1 = 200.$ <p>The cost of the second venue is given by:</p> $\text{Cost}_2 = 25x + 5x = 30x.$ <p>We need to find the value of <math>x</math> for which the costs are equal. Therefore, we set up the equation:</p> $200 = 30x.$ <p>To solve for <math>x</math>, we divide both sides of the equation by 30:</p> $x = \frac{200}{30}.$ <p>Simplifying the fraction, we get:</p> $x = \frac{20}{3}.$ <p>Therefore, the number of guests necessary for the two venues to be equal in cost is:</p> <p style="text-align: center;">10.</p>

## G.2 Problem gsm8k-644 (gold: 29)

**Question.** Steve is 60 years old. His wife is 4 years older than him. Their son is currently half as old as his mom and their son's wife is 3 years younger than her husband. How old is Steve's son's wife?

INTUITOR (wrong)	Multi-Reward (correct, 29)
<p>To solve this problem, we need to follow a systematic approach. Let's break it down step-by-step:</p> <p><b>Step 1: Determine Steve's age.</b></p> <p>Let's proceed step-by-step:</p> <p><b>Step 1: Determine Steve's age.</b></p>	<p>To determine the age of Steve's son's wife, we need to follow these steps:</p> <ol style="list-style-type: none"> <li>1. Identify the current age of Steve.</li> <li>2. Calculate the current age of Steve's wife.</li> <li>3. Determine the current age of Steve's son.</li> <li>4. Calculate the current age of Steve's son's wife.</li> </ol> <p>Let's go through each step in detail.</p> <p><b>Step 1: Identify the current age of Steve.</b> Steve is currently 60 years old.</p> <p><b>Step 2: Calculate the current age of Steve's wife.</b> Steve's wife is 4 years older than Steve. Therefore, her age is:</p> $\text{Age of Steve's wife} = \text{Age of Steve} + 4 = 60 + 4 = 64 \text{ years old.}$ <p><b>Step 3: Determine the current age of Steve's son.</b> Steve's son is currently half as old as his mom. Therefore, his age is:</p> $\text{Age of Steve's son} = \frac{\text{Age of Steve's wife}}{2} = \frac{64}{2} = 32 \text{ years old.}$ <p><b>Step 4: Calculate the current age of Steve's son's wife.</b> Steve's son's wife is 3 years younger than her husband. Therefore, her age is:</p> $\text{Age of Steve's son's wife} = \text{Age of Steve's son} - 3 = 32 - 3 = 29 \text{ years old.}$ <p>Thus, the age of Steve's son's wife is 29.</p>

**G.3 Problem gsm8k-895 (gold: 74)**

**Question.** Martin's weight is 55 kg. Carl's weight is 16 kg more than Martin's weight. Christian's weight is 8 kg more than Carl's weight. Harry is 5 kg less than Christian's weight. What is the weight of Harry, in kg?

<b>INTUITOR (wrong)</b>	<b>Multi-Reward (correct, 74)</b>
<p><i>To solve this problem, we need to follow a systematic approach. Let's break it down step-by-step:</i></p> <p><b>Step 1: Determine Carl's weight.</b></p> <p><i>Let's proceed step-by-step:</i></p> <p><b>Step 1: Determine Carl's weight.</b></p>	<p><i>To determine the weight of Harry, we need to follow a step-by-step approach. Let's break it down.</i></p> <ol style="list-style-type: none"><li><i>1. Identify Martin's weight.</i></li><li><i>2. Calculate Carl's weight.</i></li><li><i>3. Calculate Christian's weight.</i></li><li><i>4. Determine Harry's weight.</i></li></ol> <p><i>Let's go through each step in detail.</i></p> <p><b>Step 1: Identify Martin's weight.</b> <i>Martin's weight is given as 55 kg.</i></p> <p><b>Step 2: Calculate Carl's weight.</b> <i>Carl's weight is 16 kg more than Martin's weight. So, we can calculate Carl's weight as follows:</i></p> $\text{Carl's weight} = \text{Martin's weight} + 16 = 55 + 16 = 71 \text{ kg.}$ <p><b>Step 3: Calculate Christian's weight.</b> <i>Christian's weight is 8 kg more than Carl's weight. So, we can calculate Christian's weight as follows:</i></p> $\text{Christian's weight} = \text{Carl's weight} + 8 = 71 + 8 = 79 \text{ kg.}$ <p><b>Step 4: Determine Harry's weight.</b> <i>Harry's weight is 5 kg less than Christian's weight. So, we can calculate Harry's weight as follows:</i></p> $\text{Harry's weight} = \text{Christian's weight} - 5 = 79 - 5 = 74 \text{ kg.}$ <p><i>Therefore, the weight of Harry is 74 kg.</i></p>

**G.4 Problem gsm8k-561 (gold: 180)**

**Question.** If Mark weighs 150 pounds and Susan weighs 20 pounds less than Mark. And their friend Bob weighs twice as much as Susan. What is the average weight of the 3 friends?

INTUITOR (wrong)	Multi-Reward (correct, 180)
<p>To solve this problem, we need to follow a systematic approach. Let's break it down step-by-step:</p> <p><b>Step 1: Determine Susan's weight.</b></p> <p>Let's proceed step-by-step:</p> <p><b>Step 1: Determine Susan's weight.</b></p>	<p>To determine the average weight of Mark, Susan, and Bob, we need to follow these steps:</p> <ol style="list-style-type: none"> <li>1. Calculate Susan's weight.</li> <li>2. Calculate Bob's weight.</li> <li>3. Find the total weight of all three friends.</li> <li>4. Divide the total weight by the number of friends to find the average weight.</li> </ol> <p>Let's go through each step in detail.</p> <p><b>Step 1: Calculate Susan's weight.</b> Mark weighs 150 pounds. Susan weighs 20 pounds less than Mark. Therefore, we can calculate Susan's weight as follows:</p> $\text{Susan's weight} = \text{Mark's weight} - 20 = 150 - 20 = 130 \text{ pounds.}$ <p><b>Step 2: Calculate Bob's weight.</b> Bob weighs twice as much as Susan. Therefore, we can calculate Bob's weight as follows:</p> $\text{Bob's weight} = 2 \times \text{Susan's weight} = 2 \times 130 = 260 \text{ pounds.}$ <p><b>Step 3: Find the total weight of all three friends.</b> The total weight is the sum of the weights of Mark, Susan, and Bob:</p> $\text{Total weight} = 150 + 130 + 260.$ <p>Let's calculate the sum:</p> $150 + 130 = 280, \quad 280 + 260 = 540.$ <p>So, the total weight of all three friends is 540 pounds.</p> <p><b>Step 4: Divide the total weight by the number of friends to find the average weight.</b> There are 3 friends, so we divide the total weight by 3:</p> $\text{Average weight} = \frac{540}{3} = 180.$ <p>Therefore, the average weight of the three friends is 180 pounds.</p>

### G.5 Problem gsm8k-967 (gold: 30)

**Question.** Nani is 8 years old. His brother is twice his age. Nani's sister is 25% younger than him. What is the total age of all three of the family members?

INTUITOR (wrong)	Multi-Reward (correct, <span style="border: 1px solid black; padding: 0 2px;">30</span> )
<p><i>To solve this problem, we need to follow a systematic approach. Let's break it down step-by-step:</i></p> <p><b>Step 1: Determine Nani's brother's age.</b></p> <p><i>Let's proceed step-by-step:</i></p> <p><b>Step 1: Determine Nani's brother's age.</b></p>	<p><i>To determine the total age of all three family members, we need to follow these steps:</i></p> <ol style="list-style-type: none"> <li>1. <i>Identify the age of Nani.</i></li> <li>2. <i>Calculate the age of Nani's brother.</i></li> <li>3. <i>Calculate the age of Nani's sister.</i></li> <li>4. <i>Sum the ages of Nani, his brother, and his sister.</i></li> </ol> <p><i>Let's go through each step in detail.</i></p> <p><b>Step 1: Identify the age of Nani.</b> <i>Nani is 8 years old.</i></p> <p><b>Step 2: Calculate the age of Nani's brother.</b> <i>Nani's brother is twice Nani's age. So, we calculate:</i></p> $\text{Age of Nani's brother} = 2 \times \text{Age of Nani} = 2 \times 8 = 16 \text{ years.}$ <p><b>Step 3: Calculate the age of Nani's sister.</b> <i>Nani's sister is 25% younger than Nani. This means her age is 75% of Nani's age. So, we calculate:</i></p> $\text{Age of Nani's sister} = 0.75 \times \text{Age of Nani} = 0.75 \times 8 = 6 \text{ years.}$ <p><b>Step 4: Sum the ages of Nani, his brother, and his sister.</b> <i>Now, we add the ages together:</i></p> $\text{Total age} = 8 + 16 + 6 = 30.$ <p><i>Therefore, the total age of all three family members is <span style="border: 1px solid black; padding: 0 2px;">30</span>.</i></p>

**What the table shows.** INTUITOR's output is the same self-repeating template across every row: a 4–6-line preamble that announces a "step-by-step" plan and then loops "Step 1: Determine X. Let's proceed step-by-step. Step 1: Determine X." until truncation, never producing a `\boxed{}` answer. The token-level entropy of this template is in  $[0.03, 0.17]$  nats (Figure 3), which is exactly what self-certainty rewards: maximally peaked next-token distributions over a fixed string. Multi-reward trained on the same prompts, the same base model, and the same step count derives the correct answer in every case — because the cluster channel pays a non-zero reward only on consensus over the *final* answer (Equation 2), the optimizer cannot collect cluster reward by emitting a confident-but-empty template. This is the per-prompt counterpart of the complementary-failure-modes claim of Section 4.3.

## H Example completions on code-reasoning benchmarks

We complement the GSM8K analysis of Appendix G with one INTUITOR-vs-multi-reward case per code benchmark from the step-160 checkpoint of Qwen2.5-1.5B (the same checkpoint scored in Table 1). Both models are trained only on math, so both code benchmarks are out-of-distribution probes for whether the reasoning structure transfers. Both INTUITOR and multi-reward completions are reproduced *verbatim* from the saved evaluation logs (Markdown markers rendered as italics; LaTeX-style math kept as in the model output; only minor formatting such as code-fence rewrapping for column fit).

### H.1 Example from CRUXEval-O (crux-test-#675)

**Question.** You are given a Python function and an assertion containing an input to the function. Complete the assertion with a literal (no unsimplified expressions, no function calls) containing the output when executing the provided code on the given input, even if the function is incorrect or incomplete.

```
[PYTHON]
def f(nums, sort_count):
    nums.sort()
    return nums[:sort_count]
assert f([1, 2, 2, 3, 4, 5], 1) == ??
[/PYTHON]
```

**Instruction.** Please answer this question by first reasoning and then providing your answer. Present your reasoning and solution in a JSON object with "reasoning" and "answer" fields, e.g., "answer": "42". Gold answer: [1].

**INTUITOR Result (incorrect, [1]).**

To determine the output of the function  $f([1, 2, 2, 3, 4, 5], 1)$ , we need to follow these steps:

1. Sort the list  $[1, 2, 2, 3, 4, 5]$ .
2. Return the first element of the sorted list.

Let's proceed step by step.

**Step 1: Sort the list.** The given list is  $[1, 2, 2, 3, 4, 5]$ . When we sort this list, we get

$[1, 2, 2, 3, 4, 5]$ .

**Step 2: Return the first element.** The first element of the sorted list is 1.

Therefore, the output of the function  $f([1, 2, 2, 3, 4, 5], 1)$  is 1.

So, the final answer is:

[1]

**Multi-Reward Result (correct, [1]).**

To solve this problem, we need to follow these steps:

1. Understand the function  $f$ .
2. Evaluate the function with the given input.
3. Provide the output of the function.

**Step-by-Step Solution.**

**Step 1: Understand the function  $f$ .** The function  $f$  takes two parameters: `nums` and `sort_count`. It sorts the list `nums` in ascending order and then returns the first `sort_count` elements of the sorted list.

**Step 2: Evaluate the function with the given input.** The input to the function is  $f([1, 2, 2, 3, 4, 5], 1)$ . Let's break it down:

- The list `nums` is  $[1, 2, 2, 3, 4, 5]$ .
- The `sort_count` is 1.

First, we sort the list `nums` in ascending order:

$sorted\_nums = [1, 2, 2, 3, 4, 5]$ .

Next, we return the first `sort_count` elements of the sorted list. Since `sort_count` is 1, we return the first element of the sorted list:

$f([1, 2, 2, 3, 4, 5], 1) = [1]$ .

**Step 3: Provide the output of the function.** The output of the function  $f([1, 2, 2, 3, 4, 5], 1)$  is  $[1]$ .

Therefore, the assertion should be:

[1]

**What this isolates.** INTUITOR misreads the slice `nums[:sort_count]` as "the first element," dropping the list-vs-scalar distinction; the boxed token is a confident integer rather than a list. Multi-reward attends to the slice operator and emits the correct list literal. The two completions are otherwise stylistically similar—this is a one-token semantic error driven by the policy converging on the high-confidence (but wrong) "first element" reading.

## H.2 Example from LiveCodeBench v6 (abc344\_a, AtCoder)

**Question.** You will be given a question (problem specification) and will generate a correct Python program that matches the specification and passes all tests.

*Problem.* You are given a string  $S$  of lowercase English letters and the character `|`;  $S$  contains exactly two `|`'s. Remove the characters between the two `|`'s, including the `|`'s themselves, and print the resulting string.

Input

$S$

Constraints

- $S$  has length 2-100, lowercase letters and `|`.
- $S$  contains exactly two `|`'s.

Sample Input 1 `atcoder|beginner|contest`

Sample Output 1 `atcodercontest`

Sample Input 2 `|spoiler|`

Sample Output 2 (empty string)

Sample Input 3 `||xyz`

Sample Output 3 `xyz`

**Instruction.** Read the input from standard input, solve the problem, and write the answer to standard output. Enclose your code within delimiters as follows: `“python...“`. Scoring: `pass@1`, all public and private tests must pass.

**INTUITOR Result (incorrect; only the *prefix* is kept).**

*To solve the problem, we need to follow these steps:*

1. Read the input string.
2. Remove the characters between the two `|`'s.
3. Print the resulting string.

*Let's proceed step by step.*

**Step 1: Read the input string.** We will use the `input()` function to read the input string.

**Step 2: Remove the characters between the two `|`'s.** We will use string slicing to remove the characters between the two `|`'s.

**Step 3: Print the resulting string.** We will use the `print()` function to output the result.

*Here is the Python code to achieve this:*

```
# Step 1: Read the input string
input_string = input()

# Step 2: Remove the characters between the two |s
result = input_string.split('|')[0]

# Step 3: Print the resulting string
print(result)
```

*Let's run this code to see the output.*

INTUITOR's solution splits on `|` and keeps the first piece only. On the sample inputs it returns `atcoder` (vs. `atcodercontest`), the empty string (correct, by accident), and the empty string (vs. `xyz`). Two of three public tests fail; the submission is scored 0.

**Multi-Reward Result (correct).**

*To solve the problem, we need to follow these steps:*

1. Read the input string  $S$ .
2. Find the positions of the two  $|$  characters.
3. Remove the characters between these two  $|$  characters.
4. Print the resulting string.

Here is the Python code that implements these steps:

```
# Read the input string
S = input()

# Find the positions of the two '|'
left_index = S.find('|')
right_index = S.rfind('|')

# Remove the characters between the two '|'
result = S[:left_index] + S[right_index + 1:]

# Print the resulting string
print(result)
```

Let's break down the code:

1. **Read the input string:** The `input()` function reads the input from the standard input.
2. **Find the positions of the two  $|$  characters:** The `find()` method is used to find the first occurrence of the character  $|$  in the string  $S$ , and the `rfind()` method is used to find the last occurrence of the character  $|$  in the string  $S$ .
3. **Remove the characters between the two  $|$  characters:** The string slicing `S[:left_index] + S[right_index + 1:]` is used to remove the characters between the two  $|$  characters.
4. **Print the resulting string:** The `print()` function is used to print the resulting string.

When you run this code with the provided sample inputs, it will correctly remove the characters between the two  $|$  characters and print the resulting string.

This passes all three public tests and the private tests (pass@1 = 1.0).

**What this isolates.** The semantic gap is precisely the operative phrase "between the two  $|$ 's." INTUITOR's proposed plan announces this requirement but its emitted code only consumes the prefix before the first  $|$ —a high-confidence but logically truncated implementation, the same pattern as the GSM8K examples in Appendix G. Multi-reward keeps both delimiter positions and emits a slice that satisfies all three sample I/O cases. Because all rollouts must agree on the final answer for the cluster channel to pay reward, the optimizer cannot collect cluster reward via the truncated-plan template that INTUITOR collapses to.